Available online at www.sciencedirect.com
SCIENCE DIRECT®
Journal of the European Ceramic Society 25 (2005) 1373–1380
www.elsevier.com/locate/jeurceramsoc

Phase diagram of the Al_2O_3–ZrO_2–La_2O_3 system

S.M. Lakiza*, L.M. Lopato

Frantsevich Institute for Materials Science Problems, Krzizanovsky 3, 03142 Kyiv, Ukraine

Available online 23 February 2005

Abstract

The phase diagram of the Al_2O_3–ZrO_2–La_2O_3 system was constructed in the temperature range 1250–2800 °C. The liquidus surface of the phase diagram reflects the preferentially eutectic interaction in the system. Three new ternary and two new binary eutectics were found. The minimum melting temperature is 1665 °C and it corresponds to the ternary eutectic $LaAlO_3$ + T-ZrO_2 + $La_2O_3{\cdot}11Al_2O_3$. The solidus surface projection and the schematic of the alloy crystallization path confirm the preferentially congruent character of phase interaction in the ternary system. The polythermal sections present the complete phase diagram of the Al_2O_3–ZrO_2–La_2O_3 system. No ternary compounds or regions of remarkable solid solution were found in the components or binaries in this ternary system. The latter fact is the theoretical basis for creating new composite ceramics with favorable properties in the Al_2O_3–ZrO_2–La_2O_3 system.

Keywords: Phase diagram; Al_2O_3; ZrO_2

1. Introduction

The Al_2O_3–ZrO_2–La_2O_3 system consists of compounds widely known as high-performance ceramic materials. An accurate phase diagram of this system is necessary for the successful development of these materials.

The phase diagrams of the bounding binary systems have been examined in some detail.[1–8] The Al_2O_3–ZrO_2 system is of the eutectic type and is described elswhere.[1] The ZrO_2–La_2O_3 system is one with limited mutual solubility of the components in the solid state.[2–4] A congruently melting compound $La_2Zr_2O_7$ (LZ_2) of a pyrochlore-type structure was found in this system. It also has rather wide temperature dependent solubility region. The phase LZ_2 forms eutectics with the components. The cubic fluorite-like (F)⇆tetragonal (T)⇆monoclinic (M) phase transformations of ZrO_2 and high temperature cubic (X)⇆ high temperature hexagonal (H)⇆low temperature hexagonal (A) phase transformations of La_2O_3 take place in the solid state and are not seen on the liquidus curves. The Al_2O_3–La_2O_3 system[5–7] includes two compounds: congruently melting at 2100 °C $LaAlO_3$ (LA) with perovskite-like structure and incongruently melting $La_2O_3{\cdot}11Al_2O_3$ (β-phase) with hexagonal structure. The phase R (80 mol.% La_2O_3) was discovered to be orthorhombic and unstable.[6,8] No solubility regions on the base of the components and binary compounds were found in the Al_2O_3–La_2O_3 system. The phase transformations of La_2O_3 X ⇆ H ⇆ A display on the liquidus curve as metatectic points at 2140 °C, 89 mol.% La_2O_3, 2050 °C, 85 mol.% La_2O_3, respectively.[5,6]

The phase diagram of the Al_2O_3–ZrO_2–La_2O_3 system has not been sufficiently studied. Subsolidus relations only were established.[9] No ternary compounds were found in the system and its triangulation was defined by LZ_2 phase, which equilibrates with phases LA, Al_2O_3 (AL) and, evidently, β-phase. In this paper the results of reinvestigation of some features of the binary bounding system ZrO_2–La_2O_3 and Al_2O_3–ZrO_2–La_2O_3 phase diagram investigation are presented as isothermal sections at 1250 and 1650 °C, liquidus and solidus projections on the concentration triangle, phase diagrams of the triangulating sections, schematic of the reactions proceeding during equilibrium crystallization of melted samples and three isopleths in a wide range of temperatures and concentrations.

* Corresponding author.
E-mail address: sergij_lakiza@ukr.net (S.M. Lakiza).

0955-2219/$ – see front matter
doi:10.1016/j.jeurceramsoc.2005.01.014

2. Experimental details

Specimens were obtained by both chemical method and from melting the component oxides. Powders of alumina (99.9%; Donetskij zavod khimreaktiviv, Donetsk), zirconia (99.99%; Donetskij zavod khimreaktiviv, Donetsk), lanthana (Laod OST-48-194-81) were used as raw materials. The appropriate quantities of oxides were blended in an agate mortar with ethanol, dried and pressed into pellets 5 mm in diameter and 5 mm in height.

Powders of $Al(NO_3)_3 \cdot 9H_2O$, $ZrO(NO_3)_2 \cdot 2H_2O$ with purity 99.9% (Donetskij zavod khimreaktiviv, Donetsk) and lanthana (Laod OST-48-194-81) were used for chemical route preparations. Both salts and lanthana were dissolved in water with some droplets of concentrated nitric acid added, dried, calcined at 900 °C in air and pressed into pellets of the same dimensions. The specimens were taken at 5–10 mol.% intervals on the two isopleths: 20 and 60 mol.% ZrO_2, on the bisector with a Al_2O_3/ZrO_2 ratio of 1, and along two sections: $LaAlO_3$–ZrO_2 and $LaAlO_3$–$La_2Zr_2O_7$. Additional compositions were chosen in the process of identifying the location of the ternary eutectic points. For the constructing of isothermal sections chemically derived samples were annealed at 1250 and 1650 °C for the time necessary to attain equilibrium, established by unchanging XRD patterns. Other samples were fired at 1250 °C in air for 6 h then melted in molybdenum pots in a DTA device[10] at total pressure of H_2 about 1.2 atm and annealed below the solidus temperature for 1 h. The specimens were investigated by X-ray (DRON-1,5, Burevestnik, St.-Petersburg), DTA in H_2 at temperatures to 2300 °C,[10] petrographic (MIN-8 optical microscope, LOMO, St. Petersburg) and microstructure phase (ZEISS DSM982 GEMINI) analysis.

3. Results and discussion

Reinvestigation of some features of the bounding binary system ZrO_2–La_2O_3 reveled the congruently melting at 2340 °C LZ_2 phase. It forms eutectics with the components at 2315 °C, 25 mol.% La_2O_3 and 1980 °C, 62.5 mol.% La_2O_3.

Two isothermal sections at 1250 and 1650 °C were constructed incorporating literature data and the XRD results obtained (Figs. 1 and 2). They are similar and only differ in the width of phase fields. In contrast with[9] we established the principal interaction in this system is between LA phase and other phases of the system Al_2O_3–ZrO_2–La_2O_3. No ternary compounds or regions of remarkable solid solution were found in the components or binaries except small region of ternary solid solutions in the ZrO_2 corner. It appeared be-

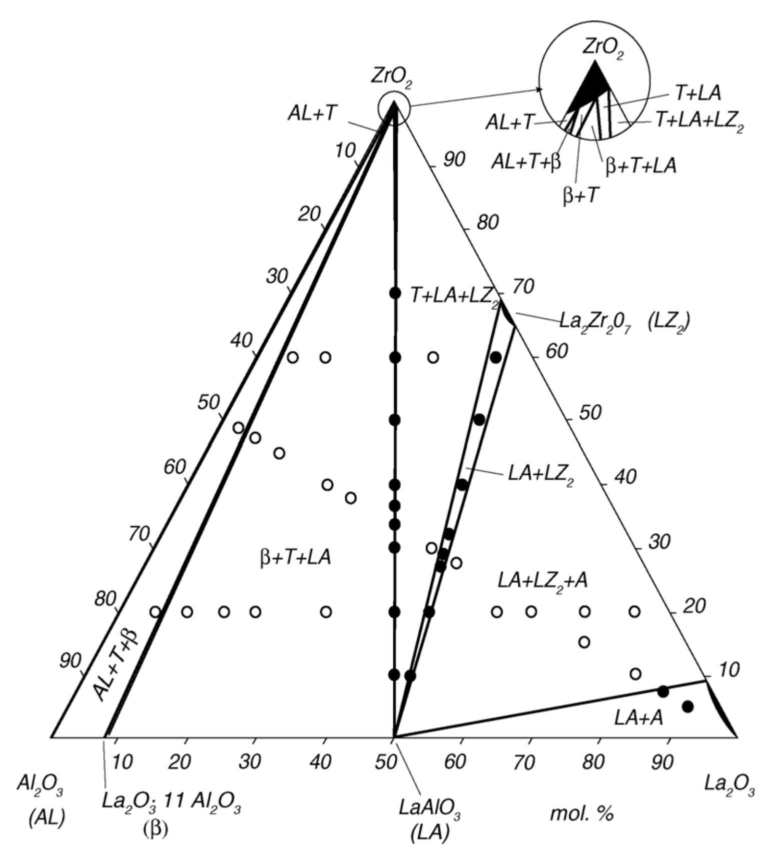

Fig. 1. Isothermal section of the Al_2O_3–ZrO_2–La_2O_3 phase diagram at 1250 °C: (●) two-phase samples; (○) three-phase samples.

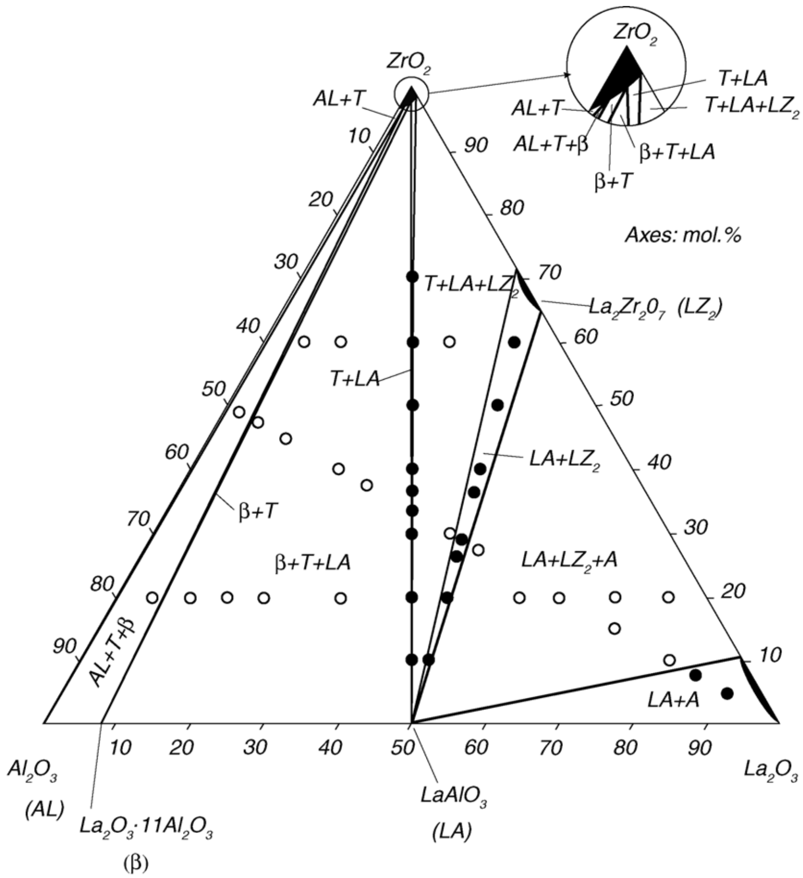

Fig. 2. Isothermal section of the Al_2O_3–ZrO_2–La_2O_3 phase diagram at 1650 °C: (●) two-phase samples; (○) three-phase samples.

cause of limited Al_2O_3 and La_2O_3 solubility in ZrO_2.[1,3] The construction of isothermal sections prognosis the following sections to be triangulating the system Al_2O_3–ZrO_2–La_2O_3: LA–LZ_2, LA–T and β–T. It should be noted that the section β–T is considered to be a partially quasibinary as far as β-phase is stable only below 1848 °C.[6] Moreover β-phase is not in equilibrium with pure ZrO_2, but solid solutions T and according to the phase equilibrium theory such section cannot be recognized as quasibinary itself.[11]

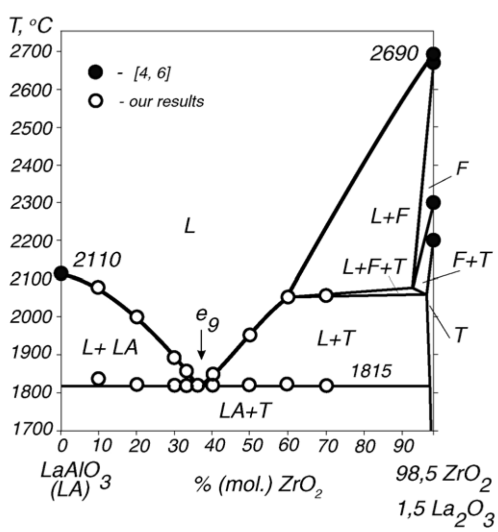

Fig. 3. Partially quazibinary section $LaAlO_3$–($1.5La_2O_3$-$98.5ZrO_2$) of the Al_2O_3–ZrO_2–La_2O_3 phase diagram.

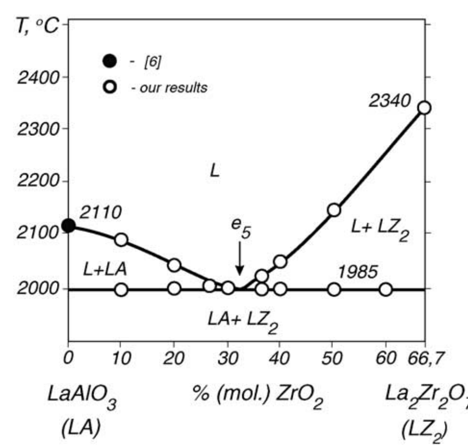

Fig. 4. Partially quasibinary section $LaAlO_3$–$La_2Zr_2O_7$ of the Al_2O_3–ZrO_2– La_2O_3 phase diagram.

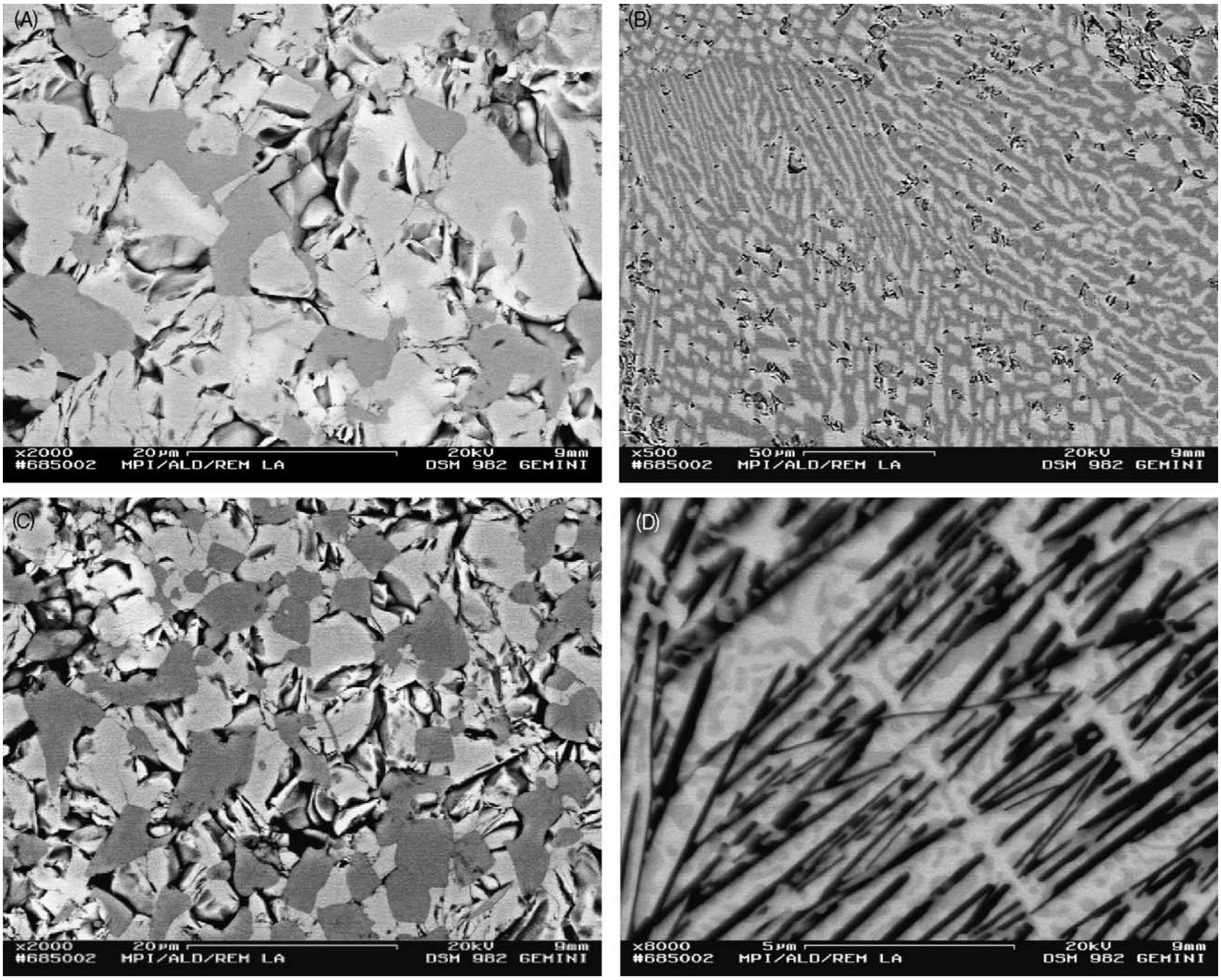

Fig. 5. Microstructures of some alloys in the system Al_2O_3–ZrO_2–La_2O_3, mol.%. Saddle points: (A) $32Al_2O_3 + 36ZrO_2 + 32La_2O_3$ (e_9): white phase, LA, grey phase, T; (B) $26Al_2O_3 + 32ZrO_2 + 42La_2O_3$ (e_5): white phase, LA, grey phase, LZ_2. Ternary invariant points: (C) $26Al_2O_3 + 36ZrO_2 + 38La_2O_3$ (E_2): white phase, LZ_2, grey phase, LA, dark grey phase, T; (D) $53Al_2O_3 + 27ZrO_2 + 20La_2O_3$ (E_3): white phase, LA, grey phase, T, black phase, β.

The triangulating Al_2O_3–ZrO_2–La_2O_3 phase diagram sections LA–T and LA–LZ_2 are shown in Figs. 3 and 4 in the temperature range 1700–2800 °C. Both sections are of the eutectic type and phase LA exhibits no solubility region. Solubility on the base of T and LZ_2 phases do not exceed 1 mol.% at ambient temperature and slowly increase with temperature.[3,4] The coordinates of eutectic points were established as (mol.%) $32Al_2O_3$–$36ZrO_2$–$32La_2O_3$, 1815 °C (e_9) and $26Al_2O_3$–$32ZrO_2$–$42La_2O_3$, 1985 °C (e_5). These eutectics were noted according to their temperature positions in the ternary system. Their microstructures are shown in Fig. 5 (A and B). At the same time these eutectic points e_9 and e_5 are saddle points in the phase diagram of the Al_2O_3–ZrO_2–La_2O_3 system (see Fig. 6). Because of the reasons mentioned above for the section β–T[11] both sections LA–LZ_2 and LA–T can also be recognized as as partially quasibinary sections of the Al_2O_3–ZrO_2–La_2O_3 phase diagram.

The liquidus surface for the Al_2O_3–ZrO_2–La_2O_3 phase diagram (Fig. 6) consists of nine fields for primary crystallization. Every component and binary compound has its own field. The largest liquidus area is occupied by solid solutions of La_2O_3 in ZrO_2. This field is divided by the monovariant line ($F \leftrightarrows T + L$) into two primary crystallization fields for solid solutions with fluorite-like cubic (F) and tetragonal (T) structures. The monoclinic form of ZrO_2 has no primary crystallization field on the liquidus because it exists at temperatures that do not exceed temperatures of binary and ternary eutectics. The ZrO_2 solid solutions in La_2O_3 with X-, H- and A-structures of rare earth oxides have their own fields for primary crystallization. As far as high-temperature phases X and H cannot be quenched from high temperatures so the coordi-

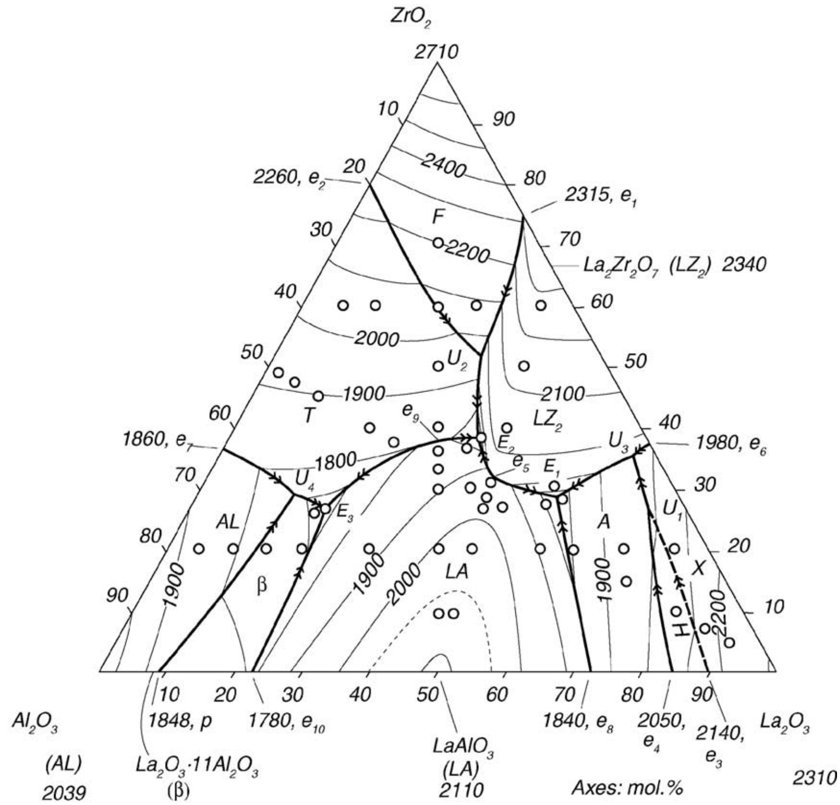

Fig. 6. Projection of the liquidus surface for the Al_2O_3–ZrO_2–La_2O_3 phase diagram.

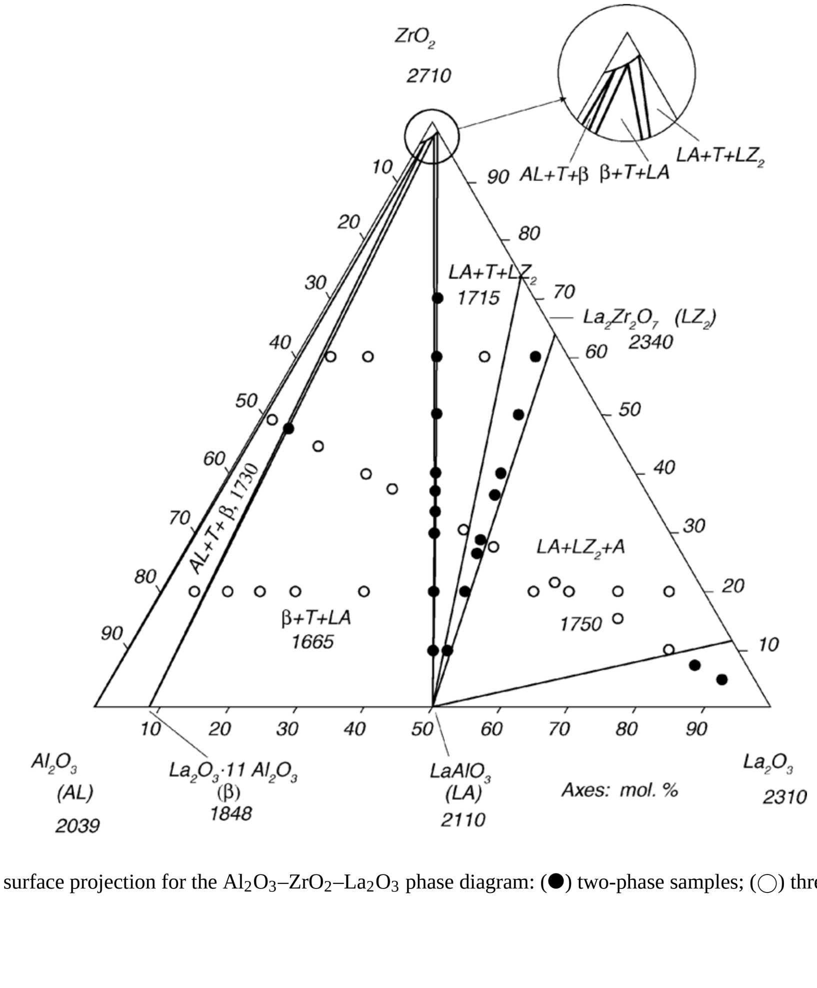

Fig. 7. Solidus surface projection for the Al_2O_3–ZrO_2–La_2O_3 phase diagram: (●) two-phase samples; (○) three-phase samples.

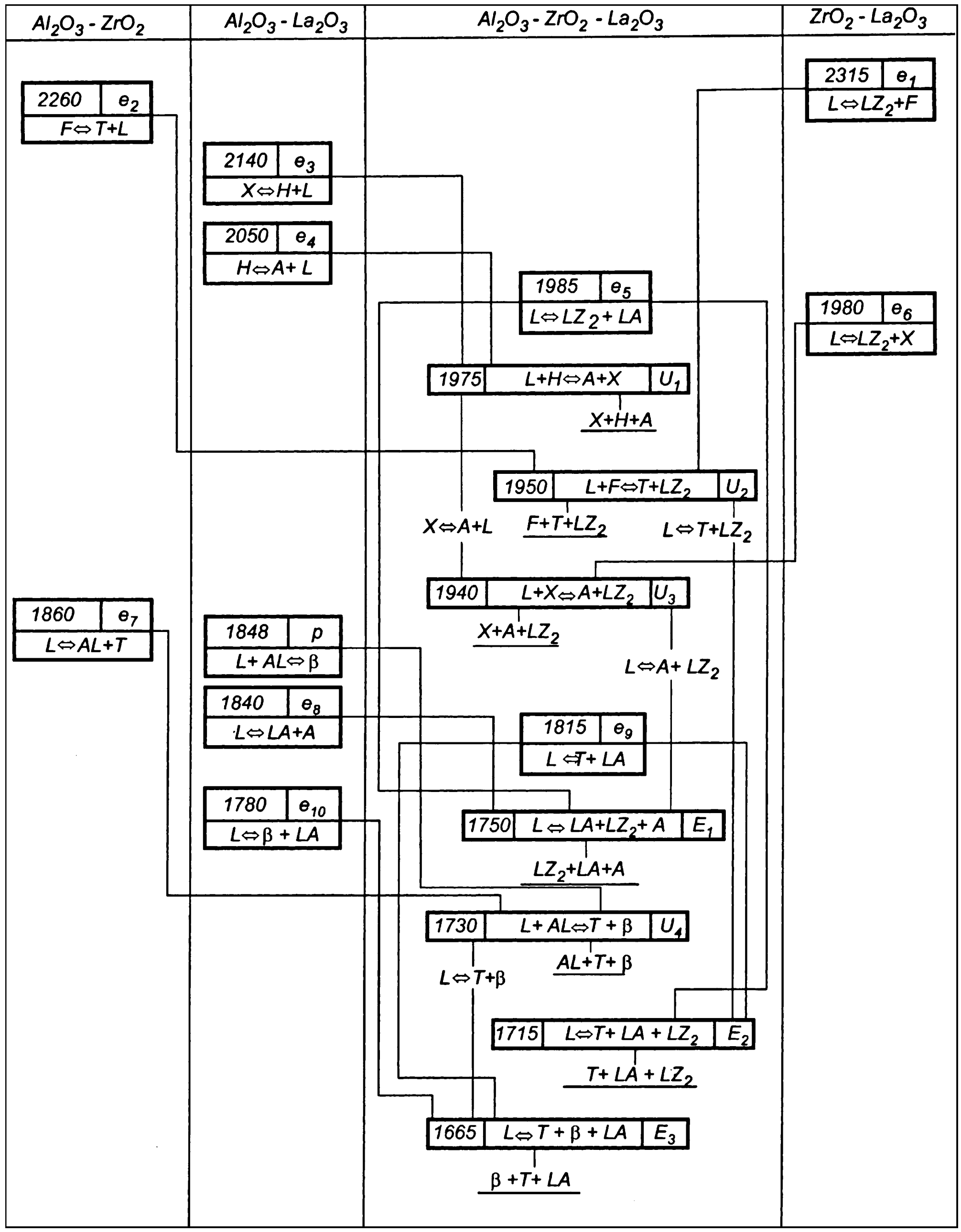

Fig. 8. Schematic of the reactions proceeding during sample crystallization in the system Al_2O_3–ZrO_2–La_2O_3.

nates of monovariant curve e_3U_1 (X ⇆ H + L) and nonvariant peritectic points U_1 and U_3 are shown tentatively. The coordinates of invariant points of the Al_2O_3–ZrO_2–La_2O_3 phase diagram are listed in Table 1. The microstructures of some invariant points are shown in Fig. 5 (C and D). It should be noted that it was impossible to make a photo of ternary eutectic E_1 because of high hydration properties of La_2O_3 that was the component of this eutectic. The minimum melting temperature in the system is 1665 °C and relates to the ternary eutectic E_3. The maximal liquidus temperature is 2710 °C and refers to the melting point of pure ZrO_2. No new phases or regions of remarkable solid solution were found in the components or binaries in the Al_2O_3–ZrO_2–La_2O_3 system.

The projection of the solidus surface of the Al_2O_3–ZrO_2–La_2O_3 phase diagram is shown in Fig. 7. Data on the coordinates of the conoid triangles of solid phases on the solidus surface were obtained from XRD measurements and are given in Table 2. According to the liquidus construction the solidus surface consists of seven isothermal three-phase fields corresponding to three invariant equilibrium of the eutectic type and four of the peritectic type. The linear surfaces representing the solidification

Table 1
Coordinates of the experimentally determined and tentative invariant points in the Al_2O_3–ZrO_2–La_2O_3 system

Equilibrium points	Temperature, (°C)	Composition, % (mol.)			Invariant equilibrium
		Al_2O_3	ZrO_2	La_2O_3	
e_5	1985	26	32	42	$L \leftrightarrows LZ_2 + LA$
U_1	1975*	5*	27*	68*	$L + H \leftrightarrows A + X$
U_2	1950	3	35	62	$L + F \leftrightarrows T + LZ_2$
U_3	1940*	18	52	30	$L + X \leftrightarrows A + LZ_2$
e_9	1815	32	36	32	$L \leftrightarrows T + LA$
E_1	1750	18	29	53	$L \leftrightarrows LZ_2 + LA + A$
U_4	1730	56	31	13	$L + AL \leftrightarrows T + \beta$
E_2	1715	26	36	38	$L \leftrightarrows T + LA + LZ_2$
E_3	1665	53	27	20	$L \leftrightarrows \beta + T + LA$

* Temperature and composition are shown tentatively.

Table 2
Coordinates of the apexes of solid phase tie-line triangles on the solidus surface of the Al_2O_3–ZrO_2–La_2O_3 phase diagram

Phase field	Compositions of equilibrium phases, mol.%					
	Al_2O_3	β	T	LA	LZ_2	A
AL + T + β	100	100	$97ZrO_2$–$0.5La_2O_3$–$2.5Al_2O_3$	–	–	–
β + T + LA	–	100	$97.5ZrO_2$–$1La_2O_3$–$1.5Al_2O_3$	100	–	–
LA + T + LZ_2	–	–	$98.5ZrO_2$–$1.5La_2O_3$	100	$74ZrO_2$–$26La_2O_3$	–
LA + LZ_2 + A	–	–	–	100	$64ZrO_2$–$36La_2O_3$	$12ZrO_2$–$88La_2O_3$

ends of the monovariant eutectics AL + T, β + T, LA + T, LA + LZ_2 and LA + A are the parts of the solidus too. Three isothermal fields LA + LZ_2 + A, LA + T + LZ_2 and β + T + LA that correspond to invariant eutectic equilibrium $L \leftrightarrows LA + LZ_2 + A$ (E_1, 1750 °C), $L \leftrightarrows LA + T + LZ_2$ (E_2, 1715 °C) and $L \leftrightarrows \beta + T + LA$ (E_3, 1665 °C), respectively, form the main solidus surface. Among four isothermal fields that correspond to invariant peritectic equilibrium the largest one is the field AL + T + β. It is the part of peritectic quadrant, where the peritectic reaction $L + AL \leftrightarrows T + \beta$ (U_4, 1730 °C) finishes with total liquid expenditure. Other three isothermal fields of peritectic origin corresponding to phase transformations of La_2O_3 ($L + H \leftrightarrows A + X$, U_1, 1975 °C; $L + X \leftrightarrows A + LZ_2$, U_3, 1940 °C) and ZrO_2 ($L + F \leftrightarrows T + LZ_2$, U_2, 1950 °C) solid solutions are degenerated. The first two are located in the La_2O_3 corner; the latter coincides with ZrO_2–La_2O_3 concentration axis in 80–95 mol.% region. On the base of data on liquidus, solidus and bounding binary systems a schematic of the reactions that proceed during the equilibrium crystallization of the Al_2O_3–ZrO_2–La_2O_3 system alloys is shown in Fig. 6. So the equilibrium alloys crystallization in this system is characterized with four in-

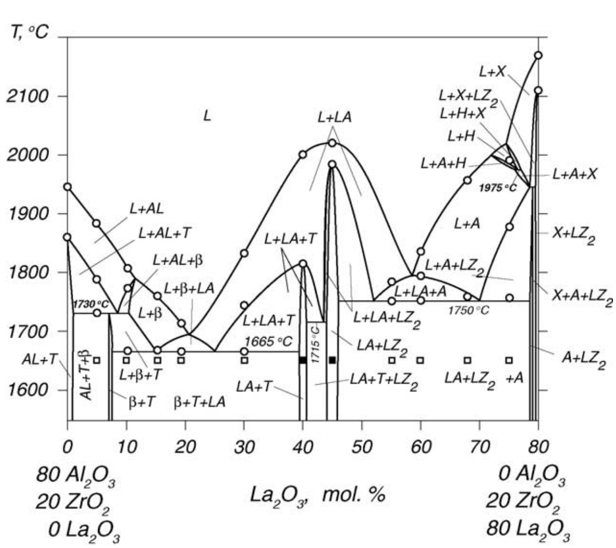

Fig. 9. Isopleth at 20 mol.% ZrO_2 for the Al_2O_3–ZrO_2–La_2O_3 phase diagram.

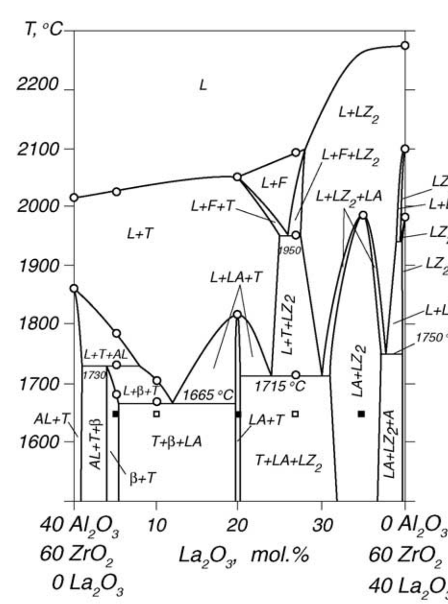

Fig. 10. Isopleth at 60 mol.% ZrO_2 for the Al_2O_3–ZrO_2–La_2O_3 phase diagram.

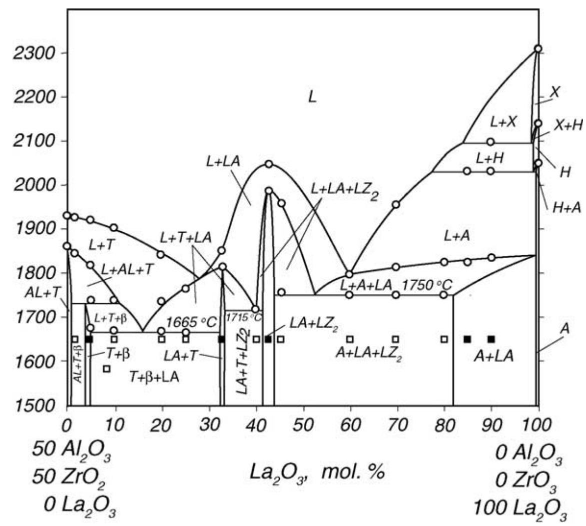

Fig. 11. Bisector $Al_2O_3/ZrO_2 = 1$ for the Al_2O_3–ZrO_2–La_2O_3 phase diagram.

variant four-phase incongruent processes at 1975 (U_1), 1950 (U_2), 1940 (U_3), 1730 °C (U_4), three invariant four-phase congruent processes at 1750 (E_1), 1715 (E_2) and 1665 °C (E_3) and two invariant three-phase congruent processes at 1985 (e_5) and 1815 °C (e_9) (Fig. 8).

Three polythermal sections were constructed to present the phase diagram of the Al_2O_3–ZrO_2–La_2O_3 system more completely: isopleths 20 and 60 mol.% ZrO_2 and bisector $Al_2O_3/ZrO_2 = 1$ (Figs. 9–11). These figures confirm the triangulation and discover the interaction in different parts of the Al_2O_3–ZrO_2–La_2O_3 phase diagram.

4. Conclusions

The phase diagram of the Al_2O_3–ZrO_2–La_2O_3 system was constructed in the temperature range 1250–2800 °C. The liquidus surface of the phase diagram reflects the preferentially eutectic interaction in the system. The minimum melting temperature is 1665 °C and it corresponds to the ternary eutectic LA + T + β. The solidus surface projection and the schematic of the alloy crystallization path confirm the preferentially congruent character of phase interaction in the ternary system. The polythermal sections present the complete phase diagram of the Al_2O_3–ZrO_2–La_2O_3 system. No ternary compounds or regions of remarkable solid solution were found in the components or binaries in this ternary system. The latter fact is the theoretical basis for creating new composite ceramics with favorable properties in the Al_2O_3–ZrO_2–La_2O_3 system.

References

1. Lakiza, S. M. and Lopato, L. M., Stable and metastable phase relations in the system Alumina–Zirconia–Yttria. *J. Am. Ceram. Soc.*, 1997, **80**, 893–902.
2. Peres, Y. and Jorba, M., ZrO_2–rare earth oxide systems. *Ann. Chim.*, 1962, **7**, 479–511.
3. Rouanet, A., Etude de la refractairite et de la structure des phases de haute temperature presentees par le systeme zircone – oxyde de lanthane. *Compt. Rendus*, 1968, **267**, 395–397, Ser. C.
4. Rouanet, A., Contribution a l’etude des systemes zircone – oxides des lanthanides au voisinage de la fusion. *Rev. Int. Hautes Temp. et Refract*, 1971, **8**, 161–180.
5. Bondar, I. A. and Vinogradova, N. V., Phase equilibria in the system lanthana – alumina. *Izv. Akad. Nauk SSSR, Ser. Chim.*, 1964(5), 785–790.
6. Mizuno, M., Berjoar, R., Coutures, J. P. and Foex, M., Phase diagram of the system Al_2O_3–La_2O_3 at elevated temperatures. *J. Ceram. Soc. Jpn.*, 1974, **82**, 631–636.
7. Ropp, R. C. and Libowitz, G. G., The nature of the alumina-rich phase in the system La_2O_3–Al_2O_3. *J. Am. Ceram. Soc.*, 1978, **61**, 473–475.
8. Yamaguchi, O., Sagiura, K., Mitsui, A. and Shimizu, K., New compound in the system La_2O_3–Al_2O_3. *J. Am. Ceram. Soc.*, 1985, **68**, C44–C45.
9. Hrovat, M., Kuscer, D., Hoic, J., Bernik, S. and Kolar, D., Preliminary data on subsolidus phase equilibria in the La_2O_3–(Al_2O_3/Fe_2O_3)–Y_2O_3 and La_2O_3–(Al_2O_3/Fe_2O_3)–ZrO_2 systems. *Mater. Sci. Lett.*, 1996, **15**, 339–342.
10. Lopato, L. M., Shevchenko, A. V. and Kuschevskij, A. E., Study of refractory oxide systems. *Powder Metallurgy*, 1972(1), 88–92.
11. Zakharov, A. M., *Phase diagrams of binary and ternary systems*. Metallurgija, Moskva, 1990, 240.